Supramolecular Influence on Keto-Enol Tautomerism and Thermochromic Properties of *o*-Hydroxy Schiff Bases

Marija Zbačnik,* Branko Kaitner

Department of Chemistry, Faculty of Science, University of Zagreb, Horvatovac 102a, HR-10000 Zagreb, Croatia
* Corresponding author's e-mail address: mzbacnik@chem.pmf.hr

Abstract: This work presents a study on thermo-optical properties of three Schiff bases (imines) in the solid state. The Schiff bases were obtained by means of mechanochemical synthesis using monosubstituted *o*-hydroxy aromatic aldehydes and monosubstituted aromatic amines. The keto-enol tautomerism and proton transfer *via* intramolecular O⋯N hydrogen bond of the reported compounds was found to be influenced more by supramolecular interactions than by a temperature change. All products were characterised by powder X-ray diffraction (PXRD), FT-IR spectroscopy, thermogravimetric (TG) analysis and differential scanning calorimetry (DSC). Molecular and crystal structures of compounds **1**, **2** and **3** were determined by single crystal X-ray diffraction (SCXRD). The molecules of **1** appear to be present as the enol-imine, the molecules of **2** as the keto-amine tautomer and the molecules of **3** exhibit keto-enol tautomeric equilibrium in the solid state. An analysis of Cambridge structural database (CSD) data on similar imines has been used for structural comparison.

**Keywords:** keto-enol tautomerism, Schiff bases, mechanochemistry, thermochromism.

INTRODUCTION

N-SUBSTITUTED imines or Schiff bases can be easily synthesized by condensation of aldehydes (or ketones) and primary amines.[1] They are a very good class of organic compounds for the investigation of faster and ecologically and economically more acceptable ways of preparation.[2,3] Many Schiff bases have been synthesized in such manner by grinding using a mortar and pestle or ball mill grinders or merely by putting the reactants in close contact and leaving the reaction mixture to age.[4–8]

The physico-chemical, biological, pharmacological properties of *N*-substituted imines and their metal complexes are well recognized reasons of a widespread and continuous strong interest in their investigation.[9,10] In this big class of compounds, *o*-hydroxy aromatic imines are drawing special attention for many years. Their optical properties in the solid state can be switched by various stimuli, for example temperature change in thermochromic or by changing the wavelength of irradiation in photochromic Schiff bases.[11] The microscopic reasons of

such macroscopic properties are still under investigation,[7,8,12–19] and this work is one of them. There are three described mutually dependant reasons for such behaviour in the solid state: proton transfer *via* intramolecular O⋯N hydrogen bonds and thus the change of the tautomeric form,[12–17] the contribution of fluorescence and not only of light absorption as a consequence of the tautomeric change and the change in molecular geometry.[18] The scientists are still trying to either reaffirm the mentioned reasons or to find imines in which the reasons cannot be strictly determined but they do show such chromic change.[7,8,18–23]

In this work, we report both the mechanochemical synthesis and the investigation of structure-thermochromism correlation of three Schiff bases (Scheme 1) derived from three aromatic aldehydes – *o*-vanillin (**ovan**), *o*-hydroxysalicylaldehyde (**oOH**) and *p*-hydroxysalicylaldehyde (**pOH**) and three aromatic amines – 2-amino-4-methylphenol (**2a4mp**), 3-amino-acetophenone (**3aa**) and 4-aminoacetophenone (**4aa**). The aldehydes and amines were selected according to the
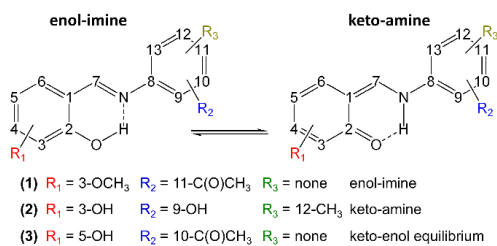
Scheme 1. Molecular structures of compounds **1**, **2** and **3** with the numbering scheme.

possibility of their substituents to participate as acceptors and/or donors in H-bonds. We have succeeded to prepare one Schiff base in enol-imine tautomeric form, compound **1**, one in keto-amine form, compound **2**, and one which exhibits keto-enol equilibrium affected by temperature change in the solid state, compound **3**.

EXPERIMENTAL

Details for synthetic procedures, PXRD, SCXRD, FT-IR, TG and DSC characterization are given in ESI.

Cambridge Structural Database[24] (CSD) Investigations

The purpose of the search was to find out how many reported Schiff bases derived from **ovan**, **oOH** and **pOH** are in keto-amine and/or in enol-imine tautomeric form in the solid state and to use the data to compare the crucial bond lengths and values of dihedral angles (Φ) with the values of compounds **1–3** and not only to use the criteria proposed by Allen *et.al.* obtained on data reported until 1987.[25] A study of the CSD Version 5.37 (November 2015 release, February 2016 Update)[24] was done using ConQuest[26] Version 1.18 and the data analysis was done using Mercury 3.8.[27] The search was made with the filtering criteria that the entries had to have their 3-D coordinates determined.

Synthesis and Characterization

In all three cases 1 mmol : 1 mmol stochiometric ratio of aldehyde and amine was used in order to obtain the Schiff base. Syntheses were performed at room temperature (RT) and at 40–60 % relative humidity. Bulk products of syntheses and recrystallization were characterized by means of PXRD, DSC, TGA and FT-IR. The structural investigations were performed at RT (298 K) and LT (110 K).

Compound **1** (1-{4-[(2-hydroxy-3-methoxy-benzyli-dene)-amino]-phenyl}-ethanone) was obtained from **ovan** and **4aa**, compound **2**, (2-hydroxy-6-[(2-hydroxy-5-methyl-phenylamino)-methylene]-cyclohexa-2,4-dienone), from **oOH** and **2a4mp** and compound **3** (1-{3-[(2,5-dihydroxy-benzylidene)-amino]-phenyl}-ethanone was obtained from **pOH** and **3aa**.

Neat grinding (**NGam**) of solid reactants (**ovan** and **4aa**) in an agate mortar lead first to a moist paste-like reaction mixture and then to an orange powder after three minutes (Figure S1a)). The paste-like intermediate phase is expected in this case since the melting points of both reactants (40–42 °C for **ovan** and 103–107 °C for **4aa**) are low enough for such behaviour and reaction pathway to take place.[7,28–33] However the conversion to compound **1** was incomplete according to the PXRD data as can be seen in Figure 1 (left). For that reason, the reaction was repeated in a mortar by means of liquid-assisted grinding (**LAGam**) using 20 µL acetonitrile (**MeCN**) yielding in complete conversion of reactants into compound **1**.

Neat grinding of **oOH** and **2a4mp** in a mortar for 11 minutes did not give any change in colour or aggrega-tion state of the reaction mixture and for that reason a catalytic amount (20 µL) of tetrahydrofuran (**thf**) was added (Figure S2a)). In three minutes of further grinding an orange powder was obtained. PXRD experiments have shown that a complete conversion of reactants to product, compound **2**, was achieved as can be seen in Figure 1 (middle). Since the melting points of both reactants are well above 100 °C (104–108 °C for **oOH** and 133–136 °C for **2a4mp**) the formation of a liquid or a paste was not expected.[7,28–33]

The reaction mixture starts to change its colour already after one minute of **NGam** of **pOH** and **3aa** (Figure S3a)). As expected from the values of the melting points of reactants (97–99 °C for **pOH** and 94–98 °C for **3aa**) the route of conversion of reactants is *via* a paste-like intermediate phase.[7,27–32] The paste forms slowly and starts to solidify after about 13 minutes of grinding. Finally, a red powder of compound **3** was obtained after 14 minutes of grinding and there were no traces of reactants in it, revealed by PXRD experiments (Figure 1 (right)).

Structural Investigations

PXRD experiments were performed on a PHILIPS PW 1840 X-ray diffractometer with Cu$K_{\alpha 1}$ (1.54056 Å) radiation at 40 mA and 40 kV. The scattered intensities were measured with a scintillation counter. The angular range (2θ) was from 5 to 45° with steps of 0.02°, and the measuring time was 0.5 s per step. The data collection and analysis were performed using the program package *Philips X'Pert*. SCXRD experiments were performed at 298 K (RT) and 110 K (LT) in order to explore thermochromic behaviour of these compounds using an Oxford Diffraction Xcalibur Kappa CCD X-ray diffractometer with graphite-monochromated MoK_{α} (λ = 0.71073 Å) radiation (for details see the ESI).

Thermal Analysis

The measurements were performed on a Mettler Toledo DSC823e and on a Mettler Toledo TGA/SDTA 851 module.
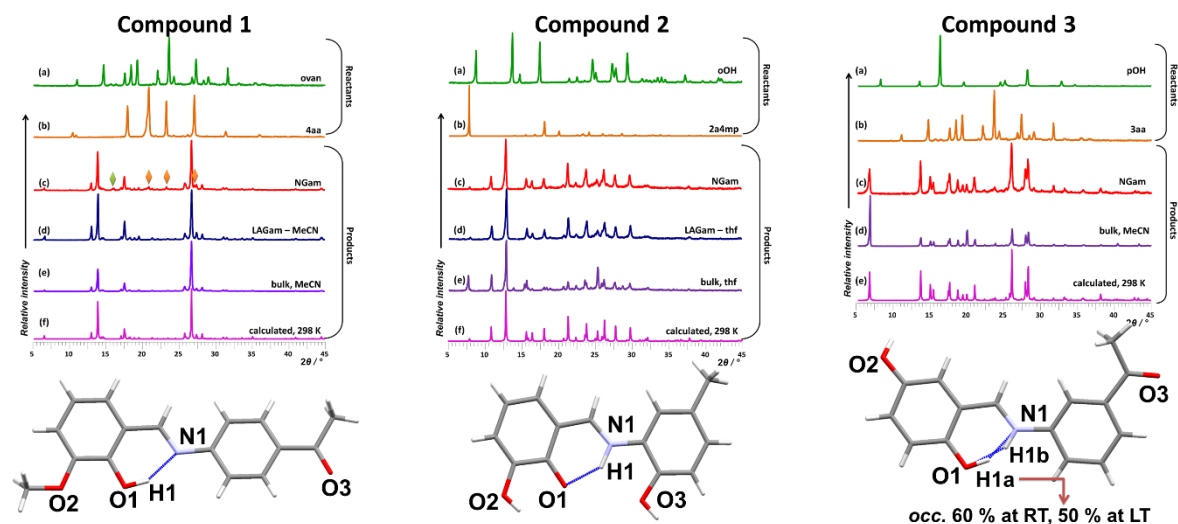
Figure 1. Molecule of compound **1** (bottom) and (top) PXRD patterns of (a) **ovan**; (b) **4aa**; (c) **1** prepared by **NG** (green and orange rhombi indicating unreacted reactants diffraction maxima); (d) **1** prepared by **LAG**; (e) **1** obtained by evaporation of **MeCN**; and (f) the calculated pattern of compound **1**. Molecule of compound **2** (bottom) and (top) PXRD patterns of (a) **oOH**; (b) **2a4mp**; (c) **2** prepared by **NG**; (d) **2** prepared by **LAG**; (e) **2** obtained by evaporation of **thf**; and (f) the calculated pattern of compound **2**. Molecule of compound **3** (bottom) and (top) PXRD patterns of (a) **pOH**; (b) **3aa**; (c) **3** prepared by **NG**; (d) **3** obtained by evaporation of **MeCN**; and (e) the calculated pattern of compound **3**.

The data was analysed using STARe Software V10.00., Mettler-Toledo AG, 1993–2011.

Spectroscopic Study on Recrystallized Material

Infrared spectra were recorded on a PerkinElmer Spectrum Two FTIR spectrophotometer using the KBr pellet method. For details see ESI.

RESULTS AND DISCUSSION

CSD[24] Data Analysis

Data obtained by means of the search are comprised in Table S6 and the structural motifs used for CSD[24] search are shown in top row of the table (see ESI).

The search revealed that there are 96 entries in total, 47 entries that correspond to Schiff bases derived from **ovan**, 40 entries for ones derived from **oOH** and 9 for **pOH**. The scatterplot of d(C7–N1) *vs.* d(C2–O1) of all data obtained by the CSD search is shown in Figure 2 while Figure 3 shows a diagram of incidence of imines being (non)planar *e.g.* having the dihedral angle ≤ 25° ≥.

Using the data reported by Allen *et. al.*[25] (Table S7 in ESI) and the data obtained by the search we can conclude that the imines derived from **ovan** (Figure 2, red dots) and **pOH** (Figure 2, green dots) are mostly in enol-imine tautomeric form in the solid state. However, the Schiff

bases derived from **oOH** (Figure 2, blue dots) in most cases have intermediary values of C2–O1 and C7–N1 bond lengths. According to the bond length criterion, compound **1** is a pure enol-imine (and is so) while compound **2** and **3** should exhibit keto-enol tautomerism in the solid state. Such behaviour was found only for compound **3** and compound **2** is a keto-amine, opposite than one can expect and conclude from Figure 2.
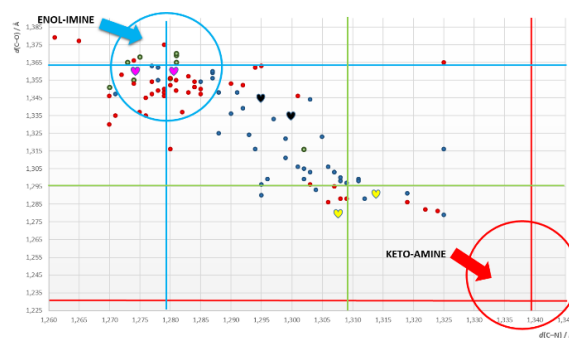
Figure 2. Scatterplot of d(C7–N1) *vs.* d(C2–O1) of data obtained by the CSD[24] search. Red dots – **ovan** imines; blue dots – **oOH** imines; green dots – **pOH** imines; pink hearts – compound **1**, yellow hearts – compound **2**; black hearts – compound **3**; blue line – limiting values of d(C7–N1) and d(C2–O1) for an enol-imine,[25] red line – limiting values of d(C7–N1) and d(C2–O1) for a keto-amine,[25] green line – average values of d(C7–N1) and d(C2–O1).[25]

In all three cases of *o*-hydroxy imines reported here, the dihedral angles between aromatic subunits are well under 25° (Table 1), the value which has been declared in literature and several times disproved as an important criterion for thermochromic behaviour.[12–23] A molecular overlay of molecules of all three Schiff bases is given in Figure 3b and shows the small deviation of the molecules from planarity. The influence of temperature on the planarity of these three imines is neglectable.

Most of the imines found reported in the CSD are planar (Table S6) and as such should show thermochromic properties, but we emphasize once again that this criterion should be taken prudently into consideration. Once again, we prove here that though the dihedral angles in molecules of **1–3** are well < 25°, compound **3** is not thermochromic.
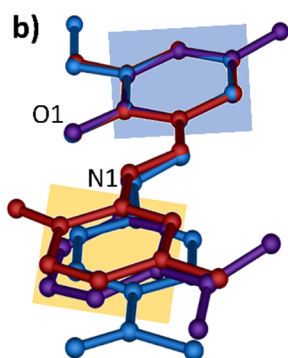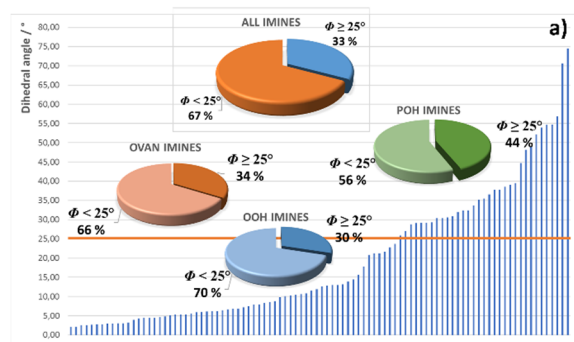
Structural Analysis

Single crystals suitable for SCXRD experiments were obtained by slow evaporation of solvent (**MeCN** for **1** and **2** and **thf** for **3**). General and crystallographic data for all three compounds are given in ESI (Tables S2-S4) and CCDC 1442712–1442714 contain crystallographic data for this paper. Table 1 comprises data on C7–N1 and C2–O1 bond

Figure 3. a) A diagram of incidence of imines being (non)planar *e.g.* having the dihedral angle ≤ 25° ≥; b) a molecular overlay of **1** (blue), **2** (red), and **3** (purple) – blue and yellow squares represent planes in which the aromatic moieties lye, hydrogen atoms were omitted for clarity.

lengths and values of dihedral angles (Φ) at RT and LT while the details on intra- and intermolecular contacts are given in Table 2 and Table 3, respectively.

Compound **1** crystallizes in monoclinic system in the general position of $P2_1/c$ space group with four molecules per unit cell. The molecular formula with the numbering scheme of **1** is given in Figure S4. As stated prior in text, the molecules of **1** are in enol-imine form both at RT and LT. The hydrogen atom H1 is located closer to the oxygen O2 atom then to the nitrogen atom N1 as can be seen in δF maps calculated through N1–C7–C1–C2–O1 chelate ring of **1** at RT and LT (Figure 4). The crystal of compound **1** changes its colour from red to yellow upon cooling (Figure 4). The values of C2–O1 and C7–N1 are also in agreement with enol-imine form at both temperatures (Table 2).

The crystal of **2** changes its colour from red at RT to orange-yellow at LT (Figure 4). The molecules of **2** crystallize in orthorhombic system, in general position of $P2_12_12_1$ space group with four molecules per unit cell. The molecular formula with the numbering scheme of **2** is given in Figure S5. The H1-atom (at both temperatures) is located closer to the N1 than to the O1 atom in the intermolecular H-bond (Figure 4). In this case the O1···N1 distance is approximately 0.045 Å shorter than in **1** (Table 2). The position of H1 indicates that the molecules of compound **2**

Table 1. C7–N1 and C2–O1 bond lengths and dihedral angle (Φ) values in compounds **1–3**.

Compound		d(C7–N1) / Å	d(C2–O1) / Å	Φ / °
1	RT	1.2740(17)	1.3566(15)	12.97(5)
	LT	1.2808(16)	1.3582(15)	11.74(4)
2	RT	1.307(5)	1.278(5)	3.9(2)
	LT	1.314(4)	1.293(4)	3.8(1)
3	RT	1.2954(18)	1.3442(17)	8.86(5)
	LT	1.2967(13)	1.3355(17)	8.27(5)

Table 2. Intramolecular O1···N1 H-bond parameters in compounds **1–3** (D = donor atom, A = acceptor atom).

	T / K	D–H···A	d(D···A) / Å	⊀(D–H···A) / °
1	298	O1–H1···N1	2.629(0)	151(1)
	110		2.625(2)	152(2)
2	298	N1–H1···O1	2.576(0)	138(1)
	110		2.588(0)	141(1)
3	298	O11–H11a···N11	2.525(2)	151(1)
				150(6)
	110	N11–H11b···O11	2.507(2)	151(5)
				150(4)

are in keto-amine tautomeric form both at RT and LT while according to Figure 2 keto-enol tautomeric equilibrium would be expected Compound **2** shows reversible thermochromic properties (Figure 4) although a bit weaker than compound **1**.

In the case of compound **3**, two molecules per unit cell crystallize in $P\bar{1}$ space group of the triclinic system. The influence of the temperature change on the colour was not found in this case, however there is an influence on the tautomeric equilibrium (Figure 4). At RT about 60 % of the molecules are in enol-imine form and 40 % in keto-amine
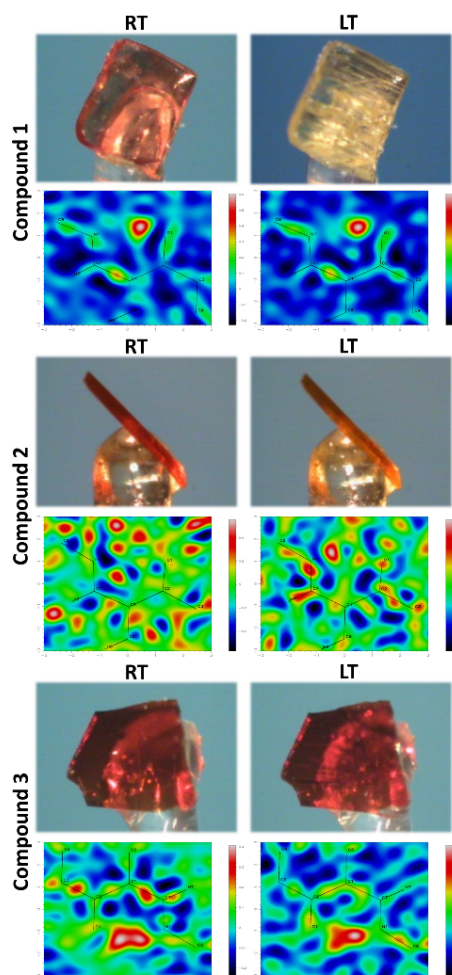
form (Figure 1). By lowering down the temperature to 110 K the position of the tautomeric equilibrium changes and about 50 % of the molecules are in enol-imine and 50 % in keto-amine form. The split position of the H1-atom in the intramolecular O1⋯N1 hydrogen bond can be easily seen in Figure 4. The C2–O1 bond length at both temperatures is on the limiting value of the intermediary and the tabulated value (ESI, Table S7) for a pure enol-imine form (Figure 2).[25] The N1–C7 bond length points to an equilibrium of both tautomers. The intramolecular H-bond is even a bit shorter than in **1** and **2** (Table 3).

Supramolecular Influences

A detailed study of the differences in crystal packing of these three Schiff bases has led us to the opinion that the thermo-optical properties and keto-enol tautomerism are governed by supramolecular influences.

Table 3. Intermolecular H-bond parameters in compounds **1**–**3** (*D* = donor atom, *A* = acceptor atom).

T / K	*D*–H⋯*A*	*d*(*D*⋯*A*) / Å	∡(*D*–H⋯*A*) / °
Compound **1**			
298	C4–H4⋯O3	3.544(2)	173.97(10)
110		3.500(2)	174.53(9)
298	C14–H14c⋯O3	3.359(2)	125.62(10)
110		3.296(2)	121.83(9)
298	C14–H14b⋯O3	3.509(2)	157.72(10)
110		3.460(2)	161.26(8)
298	C12–H12⋯O2	3.502(2)	145.79(9)
110		3.428(1)	145.28(8)
Compound **2**			
298	O2–H2⋯O1	2.619(5)	164(5)
110		2.627(4)	160(4)
298	C12–H12⋯O1	3.559(6)	121.24(34)
110		3.514(5)	122.06(23)
298	C12–H12⋯O2	3.330(7)	105.24(34)
110		3.320(5)	101.57(23)
298	C5–H5⋯O3	3.484(6)	152.37(32)
110		3.441(5)	150.34(23)
Compound **3**			
298	O2–H2⋯O1	2.683(2)	176(2)
110		2.650(2)	176(2)
298	C3–H3⋯O2	3.459(2)	126.50(9)
110		3.399(2)	126.67(9)
298	C4–H4⋯O3	3.466(2)	125.71(9)
110		3.424(2)	124.33(9)
298	C9–H9⋯O2	3.479(1)	145.46(7)
110		3.412(1)	144.76(7)
298	C15–H15b⋯O2	3.517(2)	132.73(11)
110		3.468(2)	135.87(10)

Figure 4. Photos of single crystals of compounds **1**, **2** and **3** at 298 K and 110 K. δF maps calculated through N1–C7–C1–C2–O1 chelate ring of **1**, **2** and **3**.
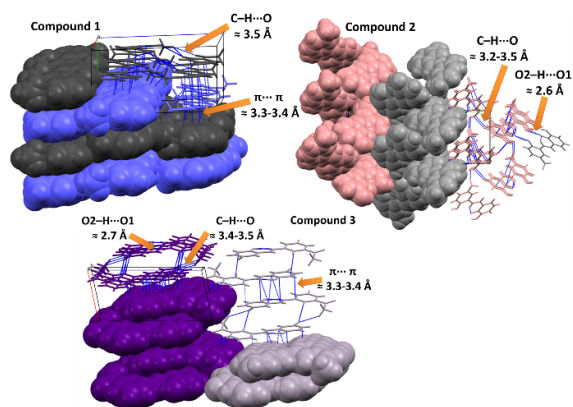
Figure 5. Packing diagrams of **1**, **2** and **3**. Interactions between molecules are highlighted.

The molecules are held together by three C–H···O3 and one C–H···O2 interaction of limiting values (Table 3) in dimers of 1D-chains formed *via* [100] direction. The π···π interactions *via* [010] direction are actually a bit shorter than the C–H···O bonds and are governing the formation of 2D-sheets as can be seen in Figure 5 The O1 atom of molecules of compound **1** does not participate in any intermolecular bonding. the enol-imine form is favoured.

The molecules of **2** form 1D-chains *via* [001] direction by means of a strong O2–H2···O1 *via* [001] direction and 2D-sheets by means of three moderate C–H···O (Table 3) interactions *via* [010]. These chains are further connected into 3D-sheets by π···π interactions (3.3–3.5 Å) *via* [001] direction (Figure 5). In this case the O1 atom participates in a strong intermolecular bond mentioned above as a hydrogen bond acceptor. That led to "pushing" the H1-atom away from the parent oxygen O1 to the N1-atom. The intramolecular N1–H1···O1 bond is just a bit shorter (Table 2) than the intermolecular O2–H2···O1

interaction. Consequently, O1 atom is under supramolecular impact resulting in keto-amine tautomeric form.

In the case of compound **3** there is a tautomeric equilibrium The O1 atom participates in O2–H2···O1 interaction as well. However, here the O2···O1 distance is a bit longer than in **2** (Table 3). This apparently facilitates the proton transfer from the parent oxygen O1 atom to the nitrogen N1 atom and *vice versa* and is crucial for the keto-enol tautomerism in this compound. The molecules of **3** form 1D-chains *via* [010] direction which are further connected into 3D-networks by means of four C–H···O (Table 3) and by π···π interactions (3.3–3.4 Å), Figure 5.

In compound **3**, the supramolecular influence is greater than in **1** and milder than in **2** and consequently keto-enol tautomeric equilibrium can be observed. The described interactions in compounds **1**–**3** can be seen in 2D-fingerprint plots obtained from Hirshfeld surfaces[34] (Figure 6).

Thermal Study

The thermal properties of the compounds were studied using DSC and TGA. This study, accompanied by PXRD experiments, revealed that compound **1** undergoes an endothermic polymorphic transition upon heating (Figure S10, S11) from form I reported here to form II. Compound **1** is stable up to 120 °C. From 121 °C to 131 °C it transforms to, for now, an unknown form,

form II, which crystallizes upon cooling to 25 °C (Figure 7). At temperatures above 132 °C the decomposition of **1** takes place at temperatures above 260 °C. The DSC curve of compound **2** has an endothermic peak with an onset at 225 °C which corresponds to melting of **2**. Starting at *approx.* 250 °C compound **2** decomposes exothermally (Figure S10, S12). Compound **3** starts to melt at 157 °C and decomposes exothermally above 200 °C (Figure S10, S13).
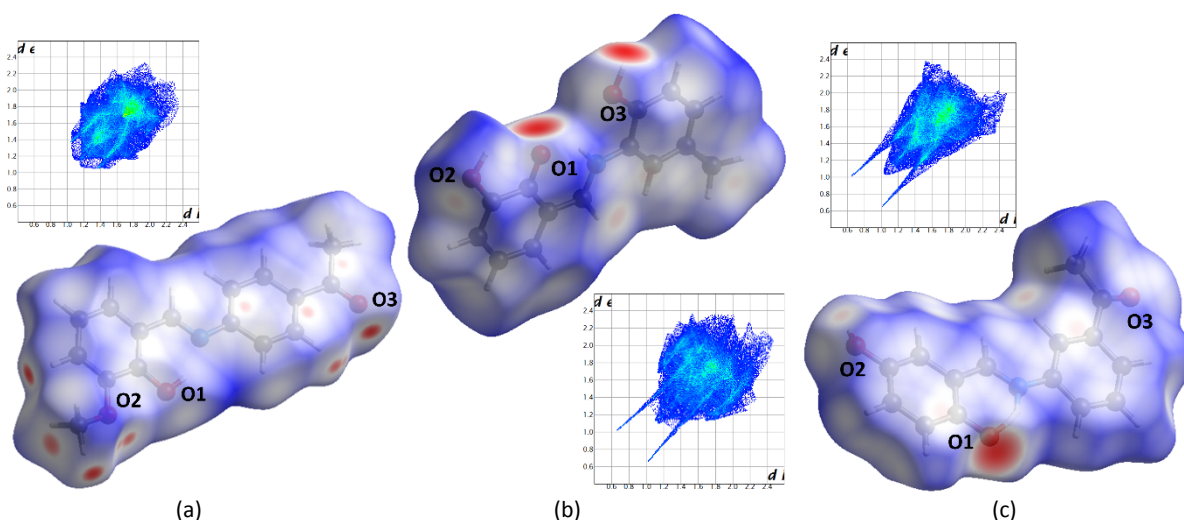
Figure 6. Hirshfeld surfaces and 2D-fingerprint plots of the molecules of (a) compound **1**; (b) **2;** and (c) **3**.
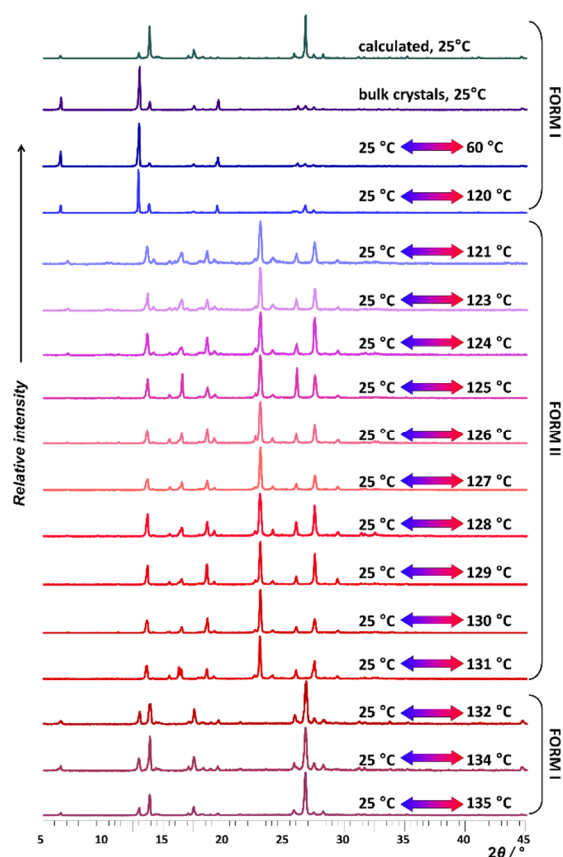
Figure 7. PXRD patterns of **1** heated up to a selected temperature and then cooled back to room temperature showing polymorphic transition at 121 °C and 131 °C.

Intermolecular interaction strength *vs.* melting point as structure-property correlation has shown to be true in the case of the three compounds reported here. Table 4 comprises the values of melting points and the values of means of d(D–H⋯A). In the case of compounds **1–3**, the smaller the value of $\bar{d}$ the higher the melting onset meaning that the number and strength of the intermolecular interactions present directly impacts on the thermal stability *i.e.* melting of the material.

According to our experience and work on numerous examples of this kind of compounds this kind of structure-property correlation should not be generalised.

Table 4. Values of $\bar{d}$(D–H⋯A) and melting onsets (t_e) in compounds **1–3** showing a good structure-property correlation.

Compound	d(D⋯A) / Å	t_e / °C
1	3.479	121
2	3.321	157
3	3.248	225

CONCLUSION

Herein, we report three *o*-hydroxy imines obtained by means of grinding. In the solid state, the molecules of compound **1** (**ovan4aa**) are in enol-imine tautomeric form, compound **2** (**oOH2a4mp**) was obtained as a keto-amine while there is a keto-enol tautomeric equilibrium in compound **3** (**pOH3aa**). The tautomerism of **1** and **2** is not influenced greatly by a temperature change although they do show thermochromic properties. On the other hand, there is a slight decrease in the population of molecules in enol-imine form with cooling but the colour change was not observed. We have demonstrated a huge effect of the type and strength of hydrogen bonds that involve the oxygen atom O1 on the keto-enol tautomerism. This has proved that the proton transfer *via* intramolecular O⋯H⋯N hydrogen bond is influenced strongly by supramolecular effects rather than by a change in molecular geometry in this type of compounds and that there is finally no doubt about the causes of keto-enol tautomerism in this class of compounds in the solid state.

The presented results are important for the understanding of supramolecular influences on macroscopic properties of imines, as well as on the possible design of other similar compounds that could be used as dyes or pigments. This study states out the importance of further research on this class of organic compounds in order to get better and detailed insight in solid-state and materials chemistry.

REFERENCES

[1] H. Schiff, *Justus Liebigs Ann. Chim.* **1864**, *131,* 118.
[2] S. L. James, C. J. Adams, C. Bolm, D. Braga, P. Collier, T. Friščić, F. Grepioni, K. D. M. Harris, G. Hyett, W. Jones, A. Krebs, J. Mack, L. Maini, A. Guy Orpen, I. P. Parkin, W. C. Shearouse, J. W. Steedk, D. C. Waddelli, *Chem. Soc. Rev.* **2012**, *41*, 413 and refences therein.
[3] J. Schmeyers, F. Toda, J. Boy, G. Kaupp, *J. Chem. Soc. Perkin Trans.* **1998**, *2*, 989.
[4] D. Cinčić, I. Brekalo, B. Kaitner, *Chem. Commun.* **2012**, *48*, 11683.
[5] K. Tanaka, F. Toda, *Chem. Rev.* **2000**, *100*, 1025.
[6] A. Carletta, J. Dubois, A. Tilborg, J. Wouters, *CrystEngComm.* **2015**, *17*, 3509.

[7]   M. Zbačnik, B. Kaitner, *CrystEngComm.* **2014**, *16*, 4162.

[8]   B. Kaitner, M. Zbačnik, *Acta Chim. Slov.* **2012**, *59*, 670.

[9]   M. Proetto, W. Liu, A. Hagenbach, U. Abram, R. Gust, *Eur. J. Med. Chem*. **2012**, *53*, 168.

[10] A. Blagus, D. Cinčić, T. Friščić, B. Kaitner, V. Stilinović, *Maced. J. Chem. Chem. Eng.* **2010**, *29*, 117.

[11] H. Bouas-Laurent, H. Durr, *Pure Appl. Chem*. **2001**, *73*, 639: Thermochromism is defined as a reversible colour change caused by a temperature change and photochromism is a reversible transformation of a chemical species induced in one or both directions by absorption of electromagnetic radiation between two forms having different absorption spectra.

[12] E. Hadjoudis, M. Vittorakis, I. M. Mavridis, *Tetrahedron* **1987**, *43*, 1345.

[13] E. Hadjoudis, I. M. Mavridis, *Chem. Soc. Rev.* **2004**, *33*, 579.

[14] M. D. Cohen, G. M. J. Schmidt, *J. Phys. Chem.* **1962**, *66*, 2442.

[15] M. D. Cohen, G. M. J. Schmidt, S. Flavian, *J. Chem. Soc.* **1964**, 2030.

[16] M. D. Cohen, Y. Hirshberg, G. M. J. Schmidt, *J. Chem. Soc.* **1964**, 2051.

[17] J. Bergman, L. Leiserowitz, G. M. J. Schmidt, *J. Chem. Soc.* **1964**, 2060.

[18] J. Harada, T. Fujiwara, K. Ogawa, *J. Am. Chem. Soc.* **2007**, *129*, 16216.

[19] K. Ogawa, Y. Kasahara, Y. Ohtani, J. Harada, *J. Am. Chem. Soc.* **1998**, *120*, 7107.

[20] F. Robert, A. D. Naik, B. Tinant, R. Robiette, Y. Garcia, *Chem. – Eur. J.* **2009**, *15*, 4327.

[21] F. Robert, P.-L. Jacquemin, B. Tinant, Y. Garcia, *CrystEngComm.* **2012**, *14*, 4396.

[22] D. A. Safin, M. Bolte, Y. Garcia, *CrystEngComm.* **2014**, *16*, 87868793.

[23] M. Zbačnik, I. Nogalo, D. Cinčić, B. Kaitner, *CrystEngComm.* **2015**, *17*, 7870.

[24] F. H. Allen, *Acta Crystallogr. B* **2002**, *58*, 380.

[25] F. H. Allen, O. Kennard, D. G. Watson, L. A. Brammer, G. Orpen, *J. Chem. Soc. Perkin Trans*. **1987**, *2*, S1.

[26] I. J. Bruno, J. C. Cole, P. R. Edgington, M. Kessler, C. F. Macrae, P. McCabe, J. Pearson, R. Taylor, *Acta Cryst. B* **2002**, *58*, 389.

[27] C. F. Macrae, P. R. Edgington, P. McCabe, E. Pidcock, G. P. Shields, R. Taylor, M. Towler, J. van de Streek, *J. Appl. Cryst*. **2006**, *39*, 453.

[28] G. Rothenberg, A. P. Downie, C. L. Raston, J. L. Scott, *J. Am. Chem. Soc.* **2001**, *123*, 8701.

[29] O. Dolotko, J. W. Wiench, K. W. Dennis, V. K. Pecharsky, V. P. Balema, *New J. Chem.* **2010**, *34*, 25.

[30] G. Kaupp, *CrystEngComm.* **2003**, *5*, 117.

[31] R. Kuroda, K. Higashiguchi, S. Hasebe, Y. Imai, *CrystEngComm.* **2004**, *6*, 463.

[32] K. Chadwick, R. Davey, W. Cross, *CrystEngComm*. **2007**, *9*, 732.

[33] A. Jayasankar, A. Somwangthanaroj, Z. J. Shao, N. Rodríguez-Hornedo, *Pharm. Res.* **2006**, *23*, 2381.

[34] J. J. McKinnon, M. A. Spackman, A. S. Mitchell, *Acta Crystallogr. Sect. B: Struct. Sci.* **2004**, *60*, 627.

SUPPORTING INFORMATION

Supramolecular influence on keto-enol tautomerism and thermochromic properties of *o*-hydroxy Schiff bases

Marija Zbačnik* and Branko Kaitner

[a]*Laboratory of General and Inorganic Chemistry, Department of Chemistry, Faculty of Science, University of Zagreb, Horvatovac 102a, HR-10002 Zagreb, Croatia*

Email: mzbacnik@chem.pmf.hr
Fax: +385 1 4606 341
Tel: +385 1 4606 379

Table of Contents

1. EXPERIMENTAL DETAILS

1.1. Materials

All reagents and solvents were purchased from commercial sources and used as received. Table S2 comprises all starting materials and solvents used for syntheses, crystallization or liquid-assisted grinding experiments.

**Table S1** Starting materials used for various experiments.

Name	Acronym	Manufacturer
Ortho-vanillin	ovan	Acros Organics
Ortho-hydroxysalicylaldehyde	oOH	Aldrich
Para-hydroxysalicylaldehyde	pOH	Aldrich
3-aminoacetophenone	3aa	Merck
4-aminoacetophenone	4aa	Merck
Acetonitrile	MeCN	J.T.Baker
Tetrahydrofuran	thf	Kemika

1.2. Mechanochemical synthesis accompanied by PXRD experiments

All grinding experiments were performed in an agate mortar at RT and 40-50 % relative humidity. The required grinding time in the agate mortar was determined empirically when the colour of the reaction mixture stopped changing. PXRD experiments were performed on all powder products obtained by grinding to check if the condensation reaction of the aldehyde and amine yielded in product.

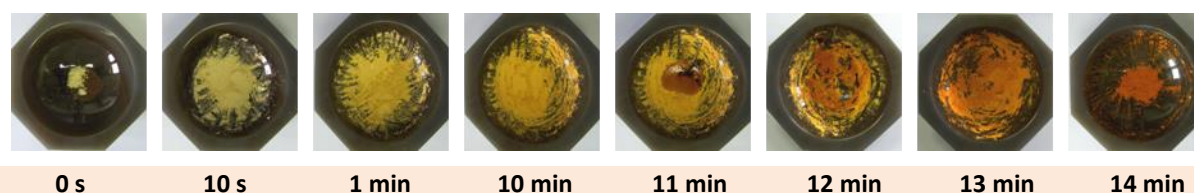### 1.2.1. Synthesis of compound 1

Equimolar quantities of **ovan** (0.153 g, 1 mmol) and **4aa** (0.135 g, 1 mmol) were first ground in an agate mortar at 25 °C. After 40 s an orange paste appears which solidifies in an orange powder after 3 minutes (Figure S1 A)). The PXRD data of that material revealed some traces of unreacted material so the reaction was repeated but by means of LAG in presence of 20 µL of **MeCN** added in the reaction mixture. Orange powder of compound **1** (**ovan4aa**) was obtained again and the PXRD data of the powder product is in good agreement with the calculated pattern. Small amount of the obtained powder was dissolved in **acn** and the single crystals suitable for SCXRD experiments were obtained by slow evaporation of solvent.

| 0 s | 10 s | 40 s | 50 s | 1 min | 1.5 min | 2 min | 3 min |
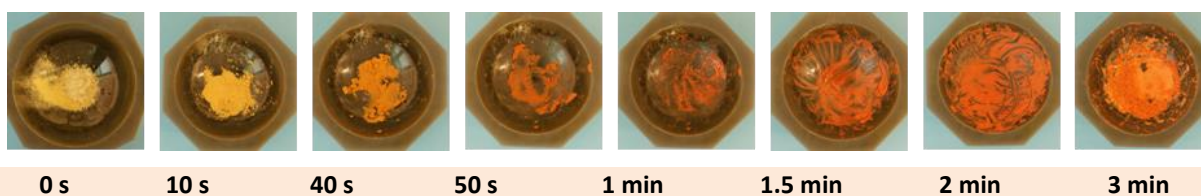
Figure S1 Neat grinding of *ovan* and **4aa** in an agate mortar.

1.2.2. Synthesis of compound **2**

Compound **2**, **oOH2a4mp**, was obtained by NG of equimolar quantities of **oOH** (0.135 g, 1 mmol) and **2a4mp** (0.123 g, 1 mmol) in an agate mortar at 25 °C for 11 minutes and the reaction mixture did not change its colour. For that reason, 20 µL of **thf** was added in the reaction mixture and the mixture started changing its colour from yellow to orange. Finally, an orange powder of compound **2** was obtained in 14 minutes of grinding in total. The PXRD data of the powder product obtained by LAG is in a good agreement with the calculated pattern. Small amount of the obtained powder was dissolved in **thf** and the single crystals suitable for SCXRD experiments were obtained by slow evaporation of solvent.

| 0 s | 10 s | 1 min | 10 min | 11 min | 12 min | 13 min | 14 min |

Figure S2 Liquid-assisted grinding of **oOH** and **2a4mp** in an agate mortar.

1.2.3. Synthesis of compound **3**

Red powder of compound **3**, **pOH3aa**, was obtained as by NG of equimolar quantities of **pOH** (0.135 g, 1 mmol) and **3aa** (0.135 g, 1 mmol) in an agate mortar at 25 °C. After about 10 minutes of grinding a red paste starts to appear and it starts to solidify in about 2 minutes. The PXRD data of the red powder product is in good agreement with the calculated pattern. Small amount of the obtained powder was dissolved in **MeCN** and the single crystals suitable for SCXRD experiments were obtained by slow evaporation of solvent.

| 0 s | 10 s | 1 min | 10 min | 11 min | 12 min | 13 min | 14 min |
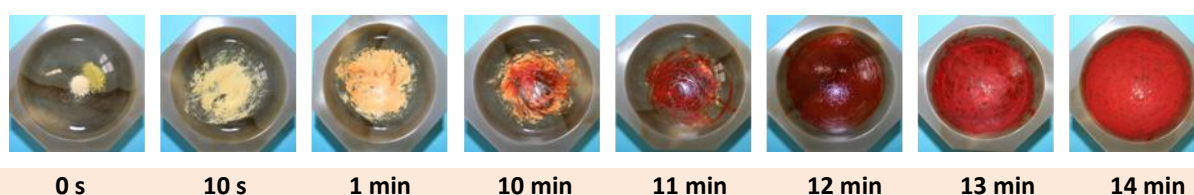
Figure S3 Neat grinding of **pOH** and **3aa** in an agate mortar.

1.3.   Powder X-Ray diffraction experiments

Powder X-ray diffraction (PXRD) experiments were performed on a PHILIPS PW 1840 X-ray diffractometer with Cu$K_{\alpha 1}$ (1.54056 Å) radiation at 40 mA and 40 kV. The scattered intensities were measured with a scintillation counter. The angular range (2θ) was from 5 to 45° with steps of 0.02°, and the measuring time was 0.5 s per step. The data collection and analysis were performed using the program package *Philips X'Pert*. [1,2,3]

1.4.   Single Crystal X-Ray diffraction experiments

Crystal and molecular structures were determined at 298 and 110 K using single crystal X-ray diffraction. Diffraction measurements were made on an Oxford Diffraction Xcalibur Kappa CCD X-ray diffractometer with graphite-monochromated MoK_α (λ = 0.71073 Å) radiation and the instrument was operated using *CrysAlis CCD* and *RED*.[4] The data sets were collected using the ω scan mode over the 2θ range up to 54°. The structures were solved by direct methods and refined using the SHELXS and SHELXL programs, respectively.[5] The structural refinement was performed on F^2 using all data. The hydrogen atoms not involved in hydrogen bonding were placed in calculated positions and treated as riding on their parent atoms [C–H = 0.93 Å and U_{iso}(H) = 1.2 U_{eq}(C); C–H = 0.97 Å and U_{iso}(H) = 1.2 U_{eq}(C)] while the others were located from the electron difference map. All calculations were performed using the WinGX crystallographic suite of programs.[6] The data concerning the results of the crystallographic experiments are listed in Table S2. Further details are available from the Cambridge Crystallographic Centre (1442712–1442714).[7] Molecular structures of compounds are presented using ORTEP-3[8] and are presented in Figures S4-S6 and their packing diagrams were prepared using Mercury.[9]

1.5.   Thermal study

1.5.1. DSC experiments

The measurements were performed on a Mettler Toledo DSC823^e module in sealed aluminium pans (40 μL), heated in flowing nitrogen (200 mL min^{-1}) at a rate of 10 °C min^{-1}. The data collection and analysis was performed using the program package STAR^e Software 9.01.[10].

Samples of compound **1**, were heated to fifteen different temperatures (60 °C, 120-135 °C) and then kept at those selected temperatures for 5 minutes as well. After that, the samples were cooled to 25 °C

and PXRD measurements on the obtained material were done revealing that form I of compound **1** undergoes a temperature induced transformation at temperatures between 121 and 131 °C.

1.5.2. TG experiments

The measurements were performed on a Mettler Toledo TGA/SDTA 851 module in sealed aluminium pans (40 μL), heated in flowing nitrogen (200 mL min^{-1}) at a rate of 10 °C min^{-1}. The data collection and analysis was performed using the program package STAR^e Software 9.01.[11].
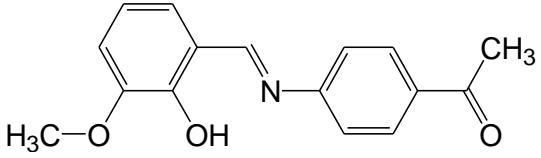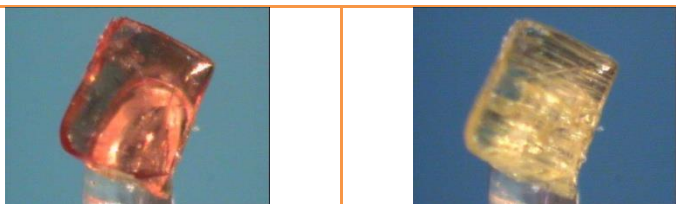
1.6. FT-IR spectroscopy

Infrared spectra were recorded on a PerkinElmer Spectrum Two FTIR spectrophotometer using the KBr pellet method. The data collection and analysis was performed using the program package PerkinElmer Spectrum 10.4.2.279[12] Table S5 comprises data for the characteristic stretching bands for **1**, **2** and **3**.
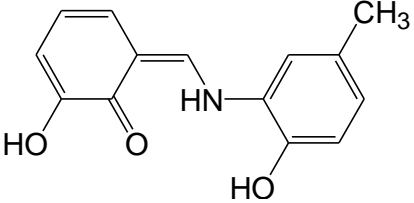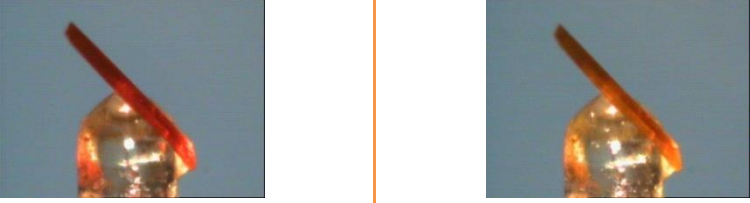
2. RESULTS

2.1. Results of SCXRD

Table S2 General and crystallographic data for **1** at 298 and 110 K.

Structural formula		
Photo		
Systematic name	1-{4-[(2-Hydroxy-3-methoxy-benzylidene)-amino]-phenyl}-ethanone	
Molecular formula	$C_{16}H_{15}NO_3$	
M_r	269.30	
Crystal system	Monoclinic	
Space group	$P\,2_1/c$	
T / K	298	110
a / Å	14.9202(8)	14.8923(9)
b / Å	6.9123(4)	6.7057(4)
c / Å	13.9675(8)	13.8901(9)
β / °	113.493(7)	113.392(7)
V / Å³	1321.10(13)	1273.10(14)
Z	4	
D_{calc} / g cm⁻³	1.354	1.405
$\lambda(K_\alpha)$ / Å	0.71073	
μ / mm⁻¹	0.094	0.098
Crystal size / mm³	0.64 x 0.52 x 0.08	
$F(000)$	568	
Refl. collected/unique	5597 / 2847	5301 / 2744
Data/Restraints/Parameters	186	
$\Delta\rho_{max}$, $\Delta\rho_{min}$ / e Å⁻³	0.181; −0.167	0.343; −0.193
$R[F^2 \geq 2\sigma(F^2)]$	0.0382	0.0372
$wR(F^2)$	0.0990	0.1057
Goodness-of-fit, S	0.815	0.902

Table S3. General and crystallographic data for **2** at 298 and 110 K.

Structural formula		
Photo		
Systematic name	2-Hydroxy-6-[(2-hydroxy-5-methyl-phenylamino)-methylene]-cyclohexa-2,4-dienone	
Molecular formula	$C_{14}H_{13}NO_3$	
M_r	243.26	
Crystal system	Orthorhombic	
Space group	$P\,2_12_12_1$	
T / K	298	110
a / Å	8.7264(10)	8.3476(9)
b / Å	22.276(2)	22.809(3)
c / Å	6.1501(7)	6.0922(6)
V / Å³	1195.5(2)	1160.0(2)
Z	4	
D_{calc} / g cm^{-3}	1.352	1.393
$\lambda(K_\alpha)$ / Å	0.71073	
μ / mm^{-1}	0.096	0.099
Crystal size / mm³	0.86 x 0.10 x 0.01	
$F(000)$	512	
Refl. collected/unique	9272 / 2536	8489 / 2515
Data/Restraints/Parameters	173	
$\Delta\rho_{max}$, $\Delta\rho_{min}$ / e Å^{-3}	0.107; −0.107	0.194; −0.205
$R[F^2 \geq 2\sigma(F^2)]$	0.0445	0.0587
$wR(F^2)$	0.0739	0.1026
Goodness-of-fit, S	0.625	0.829

Table S4. General and crystallographic data for **2** at 298 and 110 K.

Structural formula	RT occ. 60 % LT occ. 50 %	
Photo		
Systematic name	1-{3-[(2,5-Dihydroxy-benzylidene)-amino]-phenyl}-ethanone	
Molecular formula	255.27	
M_r	Triclinic	
Crystal system	$P\,\bar{1}$	
Space group	$C_{15}H_{13}NO_3$	
T / K	298	110
a / Å	6.9766(4)	6.8437(4)
b / Å	7.0995(5)	7.0600(5)
c / Å	13.5996(8)	13.5340(7)
α / °	87.879(5)	87.618(5)
β / °	79.905(5)	79.528(5)
γ / °	66.670(6)	66.455(6)
V / Å³	608.55(7)	589.14(6)
Z	2	
D_{calc} / g cm⁻³	1.393	1.439
$\lambda(K_\alpha)$ / Å	0.71073	
μ / mm⁻¹	0.098	0.101
Crystal size / mm³	0.80 x 0.62 x 0.04	
F(000)	268	
Refl. collected/unique	5123 / 2624	4682 / 2530
Data/Restraints/Parameters	180	
$\Delta\rho_{max}$, $\Delta\rho_{min}$ / e Å⁻³	0.151; −0.195	0.320; −0.204
$R[F^2 \geq 2\sigma(F^2)]$	0.0382	0.0399
$wR(F^2)$	0.0915	0.1004
Goodness-of-fit, S	0.813	0.874
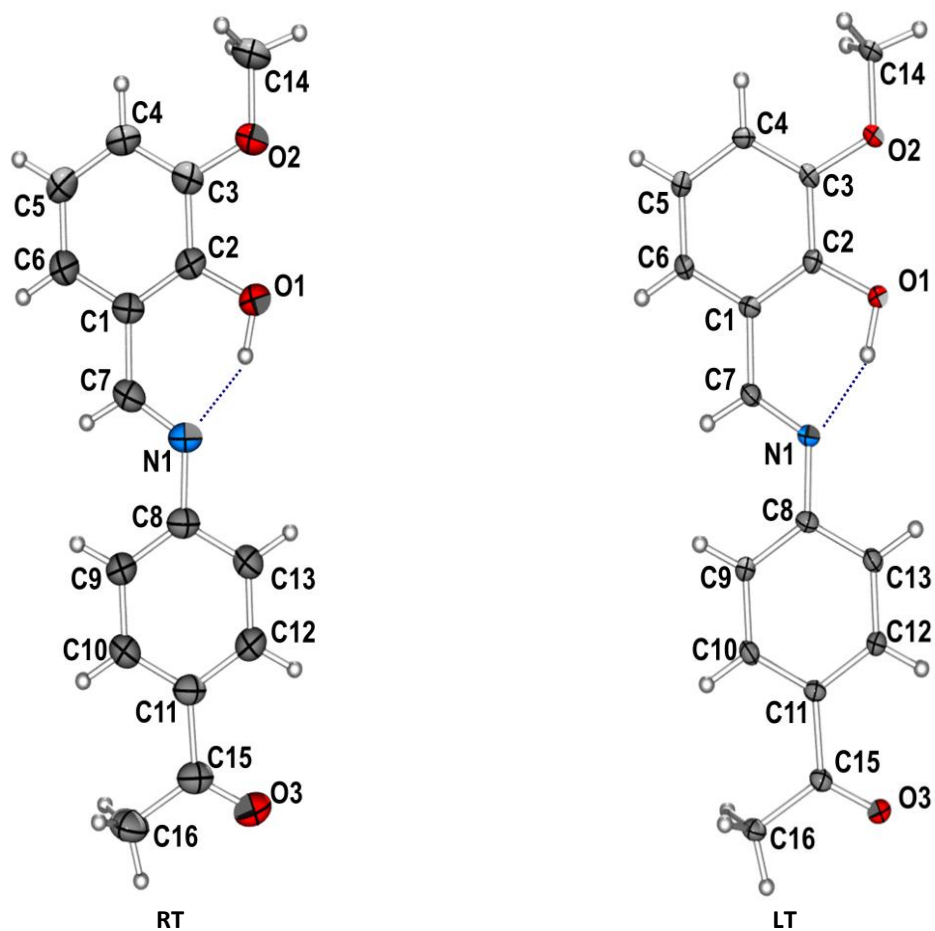
Figure S4 Thermal ellipsoid (50 %) plot of compound **1** molecule with the atom-labelling scheme. Dashed line indicates intramolecular interaction.

RT   **LT**
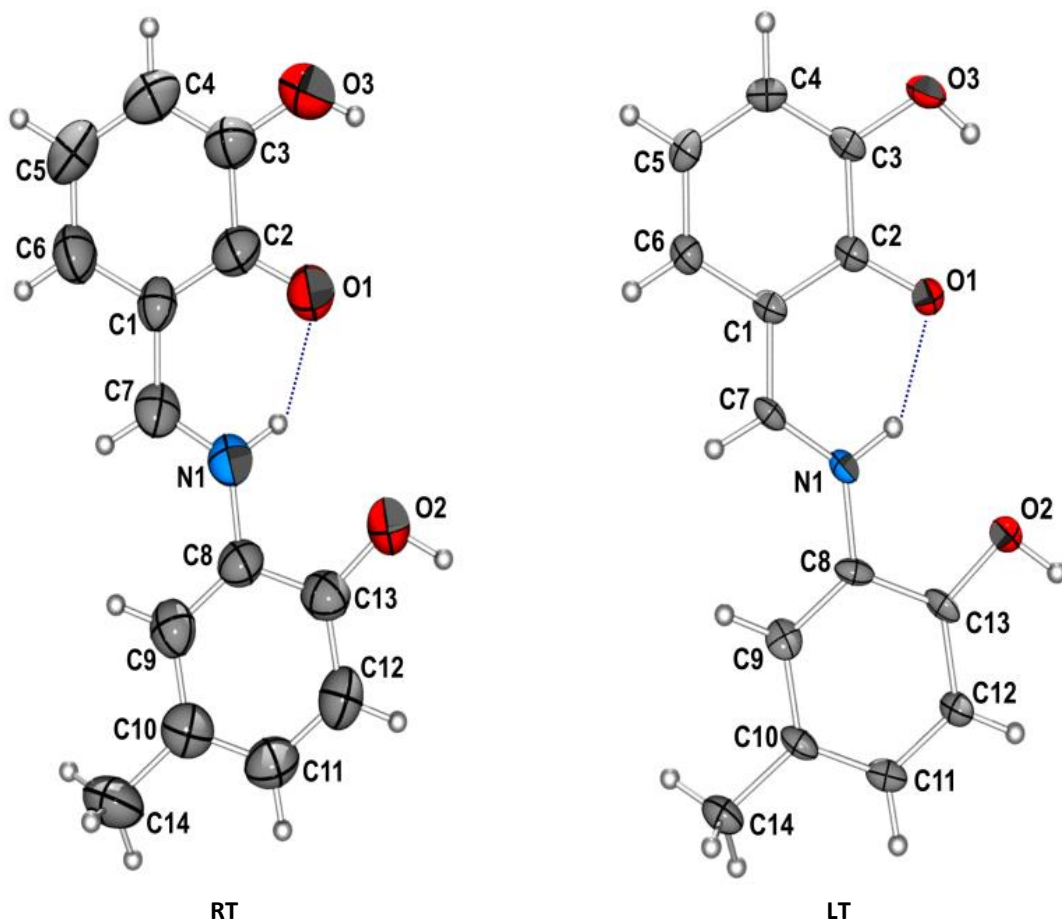
Figure S5 Thermal ellipsoid (50 %) plot of compound **2** molecule showing the atom-labelling scheme. Dashed line indicates intramolecular interaction.

RT   **LT**
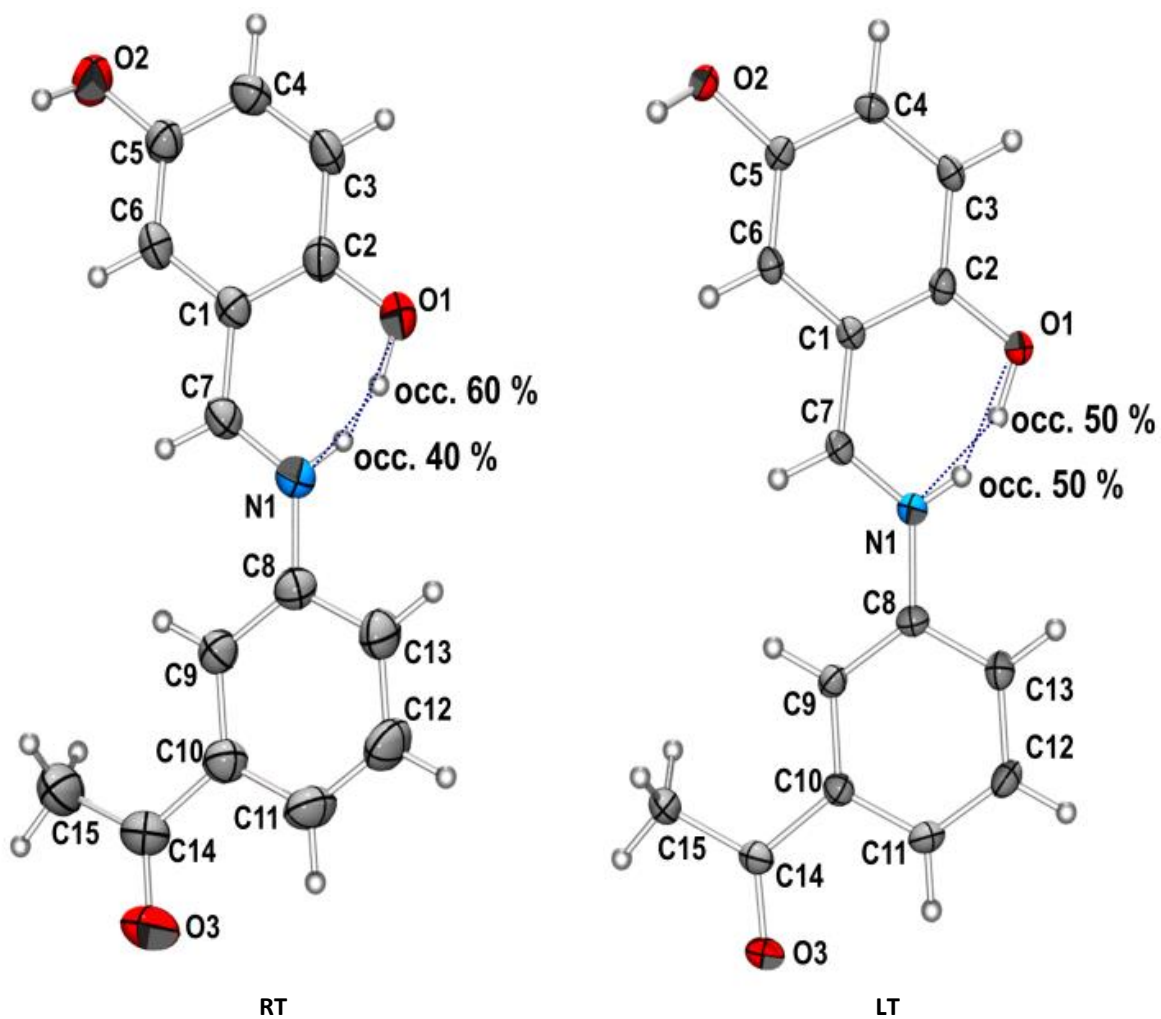
Figure S6 Thermal ellipsoid (50 %) plot of compound **3** molecule showing the atom-labelling scheme and indicating the occupancy of the hydrogen atom. Dashed line indicates intramolecular interactions.

<div align="center">
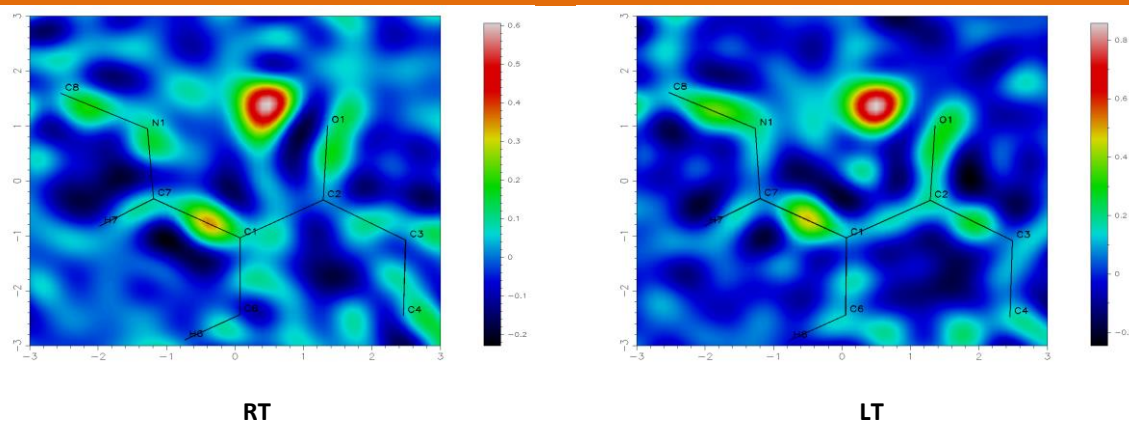
RT   **LT**
</div>

Figure S7 δF maps calculated through N1–C7–C1–C2–O1 chelate ring of **1** at RT and LT.

<div align="center">

RT   **LT**
</div>

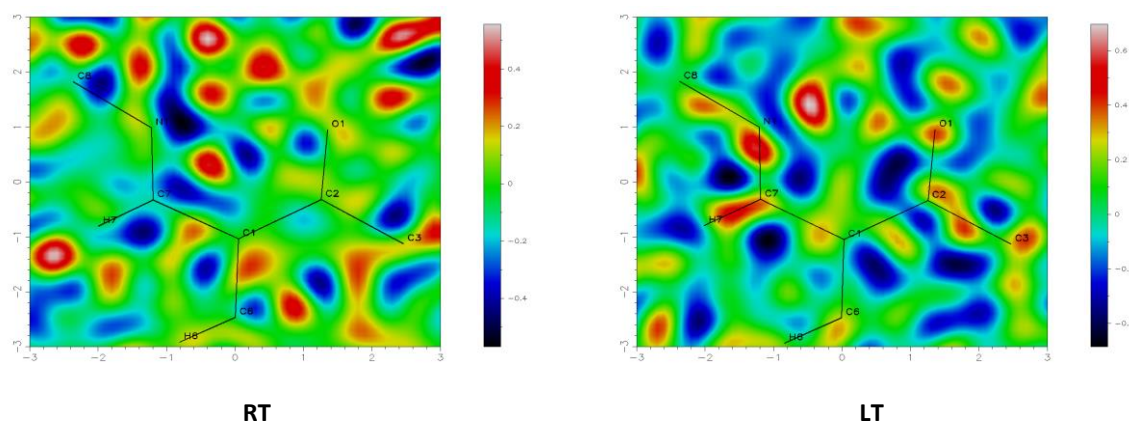**Figure S8** δF maps calculated through N1–C7–C1–C2–O1 chelate ring of **2** at RT and LT.

<div align="center">

RT   **LT**
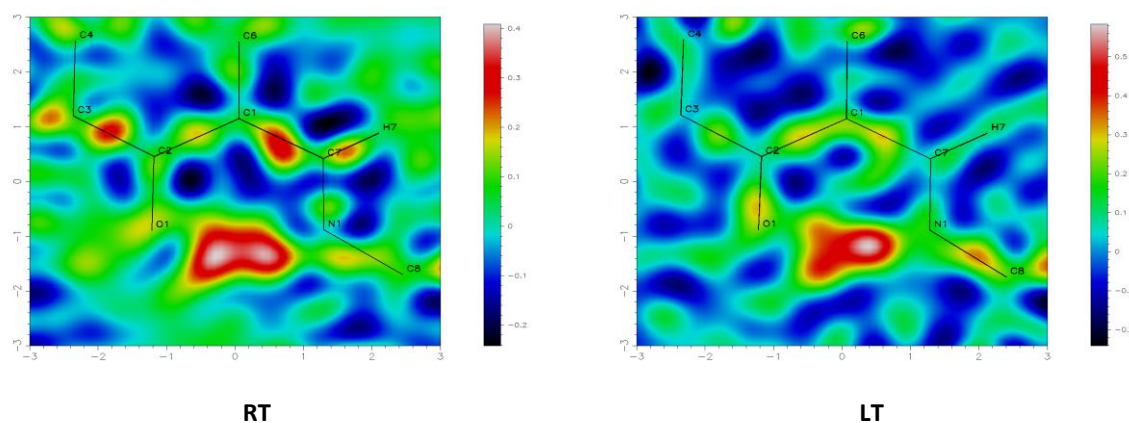</div>

Figure S9 δF maps calculated through N1–C7–C1–C2–O1 chelate ring of **3** at RT and LT.

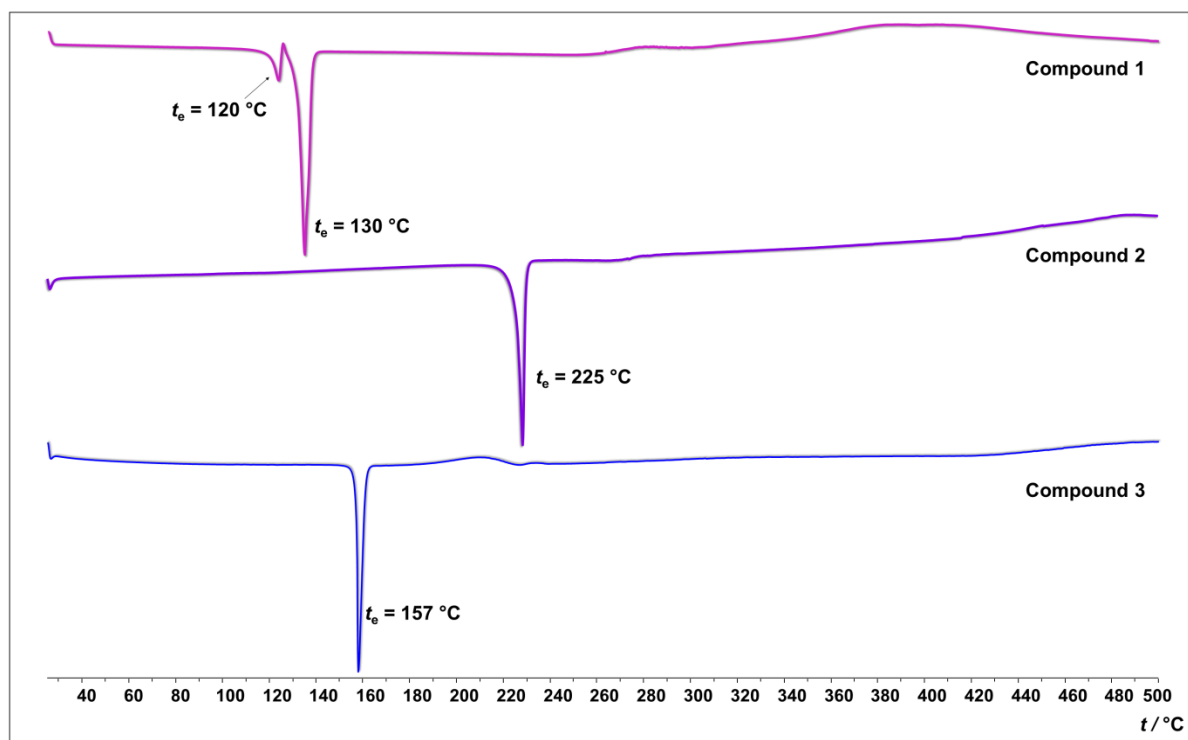## 2.4. Thermal study

Figure S10 DSC curves of recrystallized material of compound **1** (pink), **2** (purple) and **3** (blue).
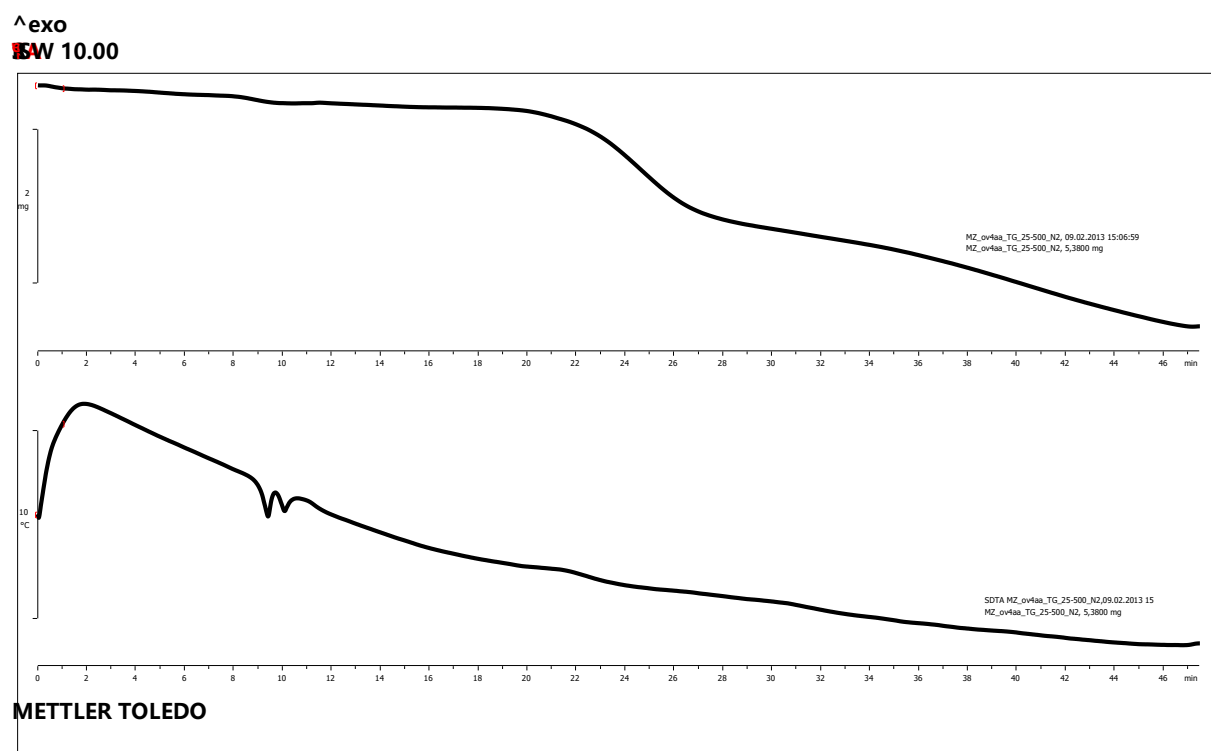

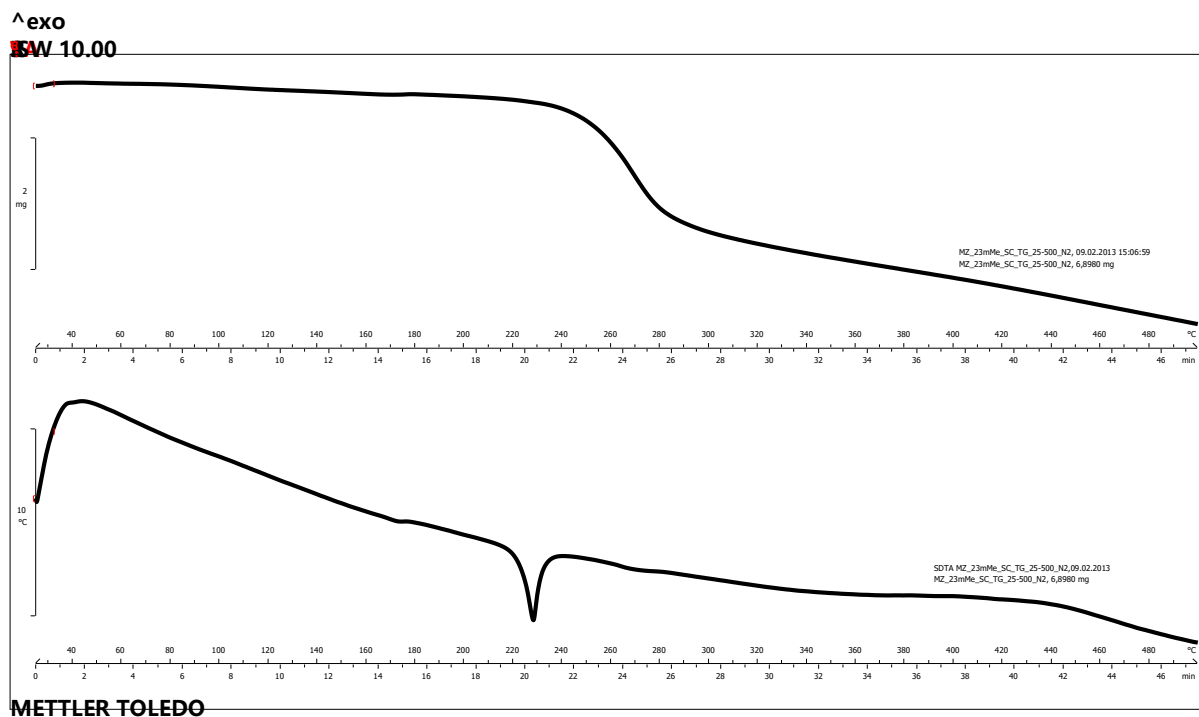**Figure S11** TGA and SDTA curves of recrystallized material of compound **1**.

Figure S12 TGA and SDTA curves of recrystallized material of compound **2**.
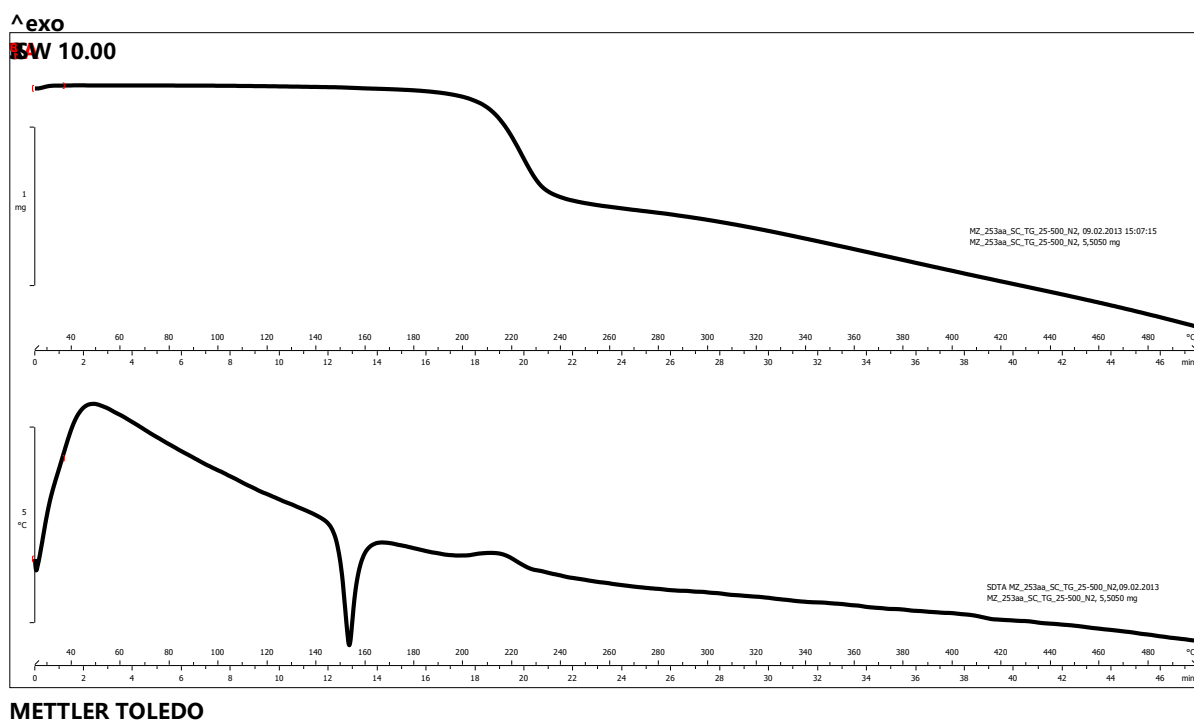
Figure S13 TGA and SDTA curves of recrystallized material of compound **3**.
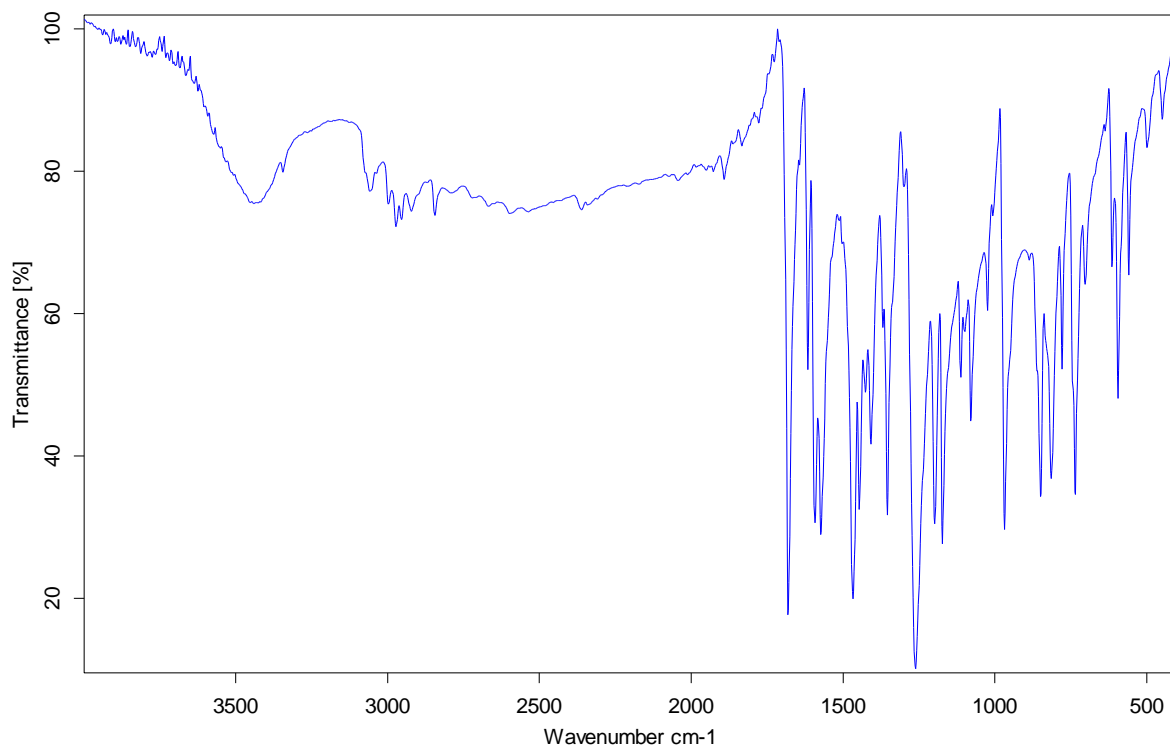
Figure S14 IR spectrum of compound **1**.
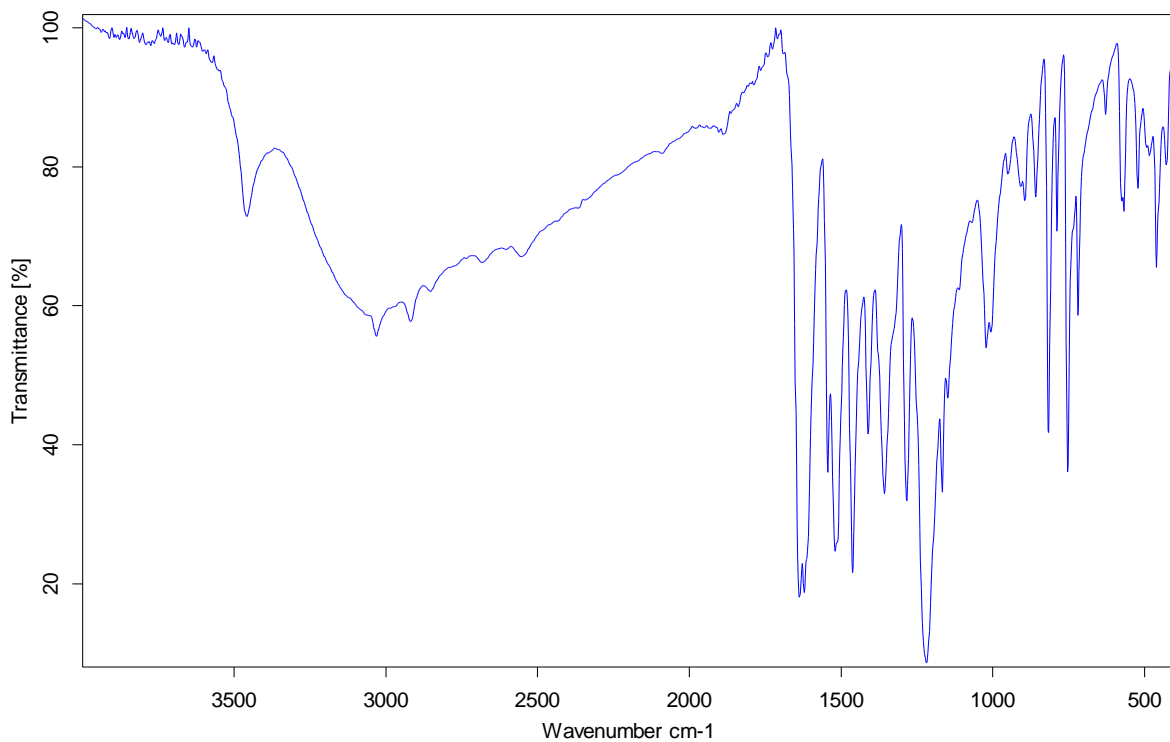
Figure S15 IR spectrum of compound **2**.
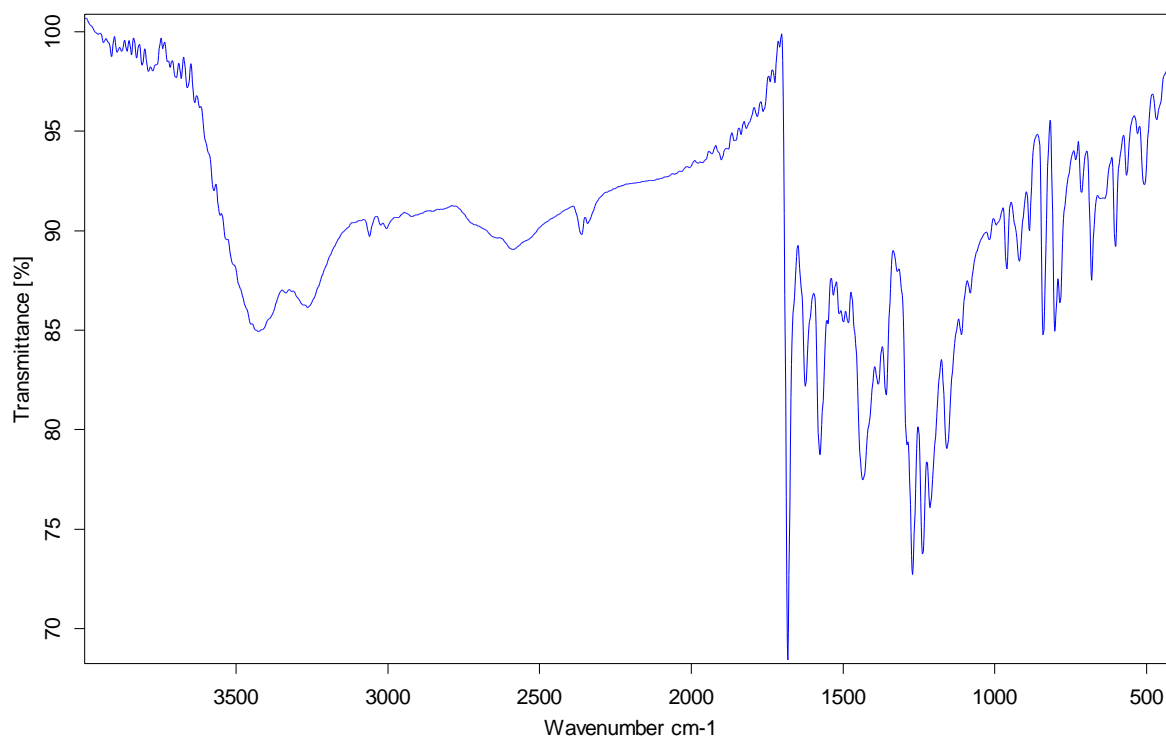
Figure S16 IR spectrum of compound **3**.
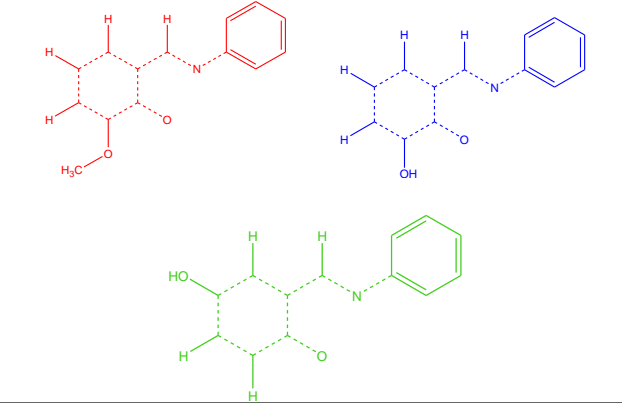
Table S5 Characteristic stretching bands for **1**, **2** and **3** found in the FT-IR spectra.

	$\widetilde{\nu}$ / cm^{-1}							
	X–H, X = N or O	C_{ar}–H, C–H	C=N	C_{ar}–O	C_{ar}– C_{ar}	C_{ar}–N	C_{ar}-O-CH$_3$	C=O
1	3442	3057, 2996	1614	1255 (1468)	1573	1357	1186	1677
2	3458	3031, 2918	1621	1462 (1284)	1543, 1519	1357		
3	3427, 3263	3061	1624	1271, 1435	1576, 1547	1358		1651

Table S6 Data obtained from the CSD on d(C7–N1), d(C2–O1) and Φ for imines derived from **ovan** (red data), **oOH** (blue data) and **pOH** (green data). Structural motifs used for searches are given in top row.

Refcode	Φ/°	d(C7–N1)/Å	d(C2–O1)/Å
AJETUF	7.451	1.274	1.355
AVUYUM	2.564	1.270	1.351
CICTOY	52.176	1.285	1.354
CIKPIW	8.522	1.281	1.369
CUCZUW	6.873	1.278	1.355
DUMSEK	21.242	1.278	1.349
DUPCIB	5.594	1.312	1.288
EKUGEW	11.941	1.301	1.346
EKUGIA	27.010	1.271	1.335
EVIMEB	53.933	1.271	1.347
EVOXIW	2.661	1.302	1.299
EVOXIW	12.944	1.288	1.325
EVOXIW01	2.607	1.308	1.300
EVOXIW01	12.631	1.299	1.322
EZUWIG	38.555	1.308	1.298
EZUWIG	39.488	1.311	1.299
EZUWIG	37.773	1.307	1.303
EZUWIG	36.565	1.302	1.305
FAGSUE	6.232	1.324	1.281
FAGSUE	7.180	1.322	1.282
FEXRIK	10.656	1.280	1.316
FEXRIK	11.510	1.265	1.377
FEXRIK01	29.200	1.283	1.348
FEXRIK01	30.860	1.279	1.350
FEXRIK01	32.406	1.284	1.351
FEXRIK01	21.672	1.272	1.358
FEXRIK02	32.339	1.277	1.347
FEXRIK02	29.175	1.279	1.348

FEXRIK02	33.682	1.279	1.348
FEXRIK02	22.808	1.274	1.353
FOCCOQ	7.933	1.304	1.293
FUGWEK	31.931	1.281	1.365
GAWKEV	12.837	1.277	1.354
GEPMIY	29.242	1.294	1.316
GETTUV	38.980	1.287	1.359
GETTUV	37.742	1.287	1.360
HAGXUJ	35.153	1.280	1.352
HUFLIE	6.173	1.303	1.303
HUFLIE	6.752	1.307	1.303
HUFLIE	23.665	1.306	1.306
IFUMAZ	5.857	1.311	1.298
IGECOM	6.737	1.279	1.346
IJENAM	7.837	1.275	1.337
IJUGUQ	70.525	1.261	1.379
KATKAS	6.142	1.319	1.291
KUFLUU	2.094	1.279	1.346
KUFLUU01	28.768	1.281	1.349
KUFLUU02	2.958	1.284	1.351
KULPOX	35.459	1.274	1.366
LOFSII	5.359	1.325	1.316
LOFSOO	6.389	1.290	1.336
MONGAZ	25.861	1.292	1.352
MONGAZ	29.076	1.290	1.353
MOYHAL	44.737	1.277	1.363
MUBKUQ	48.110	1.278	1.362
NEDMUF	8.786	1.306	1.286
NEDMUF01	3.039	1.307	1.295
NUQXAA	5.357	1.276	1.335
NUQXAA	4.870	1.283	1.357
NUQXAA01	5.352	1.282	1.337
NUQXAA01	3.233	1.294	1.362
NUQXAA02	3.952	1.276	1.345
NUQXAA03	2.130	1.280	1.356
POFWOX	3.099	1.319	1.286
QOTTEZ	10.154	1.270	1.330
QUYGOH	4.316	1.302	1.316
REZSIZ	4.464	1.291	1.348
REZSIZ01	4.437	1.288	1.348
SAPBAN	17.832	1.270	1.346
SOXGAO	2.809	1.28	1.356
SUYRIO	56.787	1.279	1.375
TEWKOX	20.885	1.309	1.288
TEWKOX01	21.254	1.308	1.288

UDURER	6.036	1.301	1.306
UDURER	12.979	1.299	1.311
UNUWEG	30.588	1.285	1.350
UNUWEG01	30.382	1.295	1.363
VEFPAZ	2.926	1.296	1.299
VIKLAD	13.211	1.303	1.296
XEYSOK	5.086	1.293	1.324
XOZJEC	30.404	1.284	1.354
XOZJUS	4.599	1.297	1.333
YALTEK	15.660	1.325	1.279
YALTEK	10.211	1.309	1.297
YAMZIW	8.375	1.295	1.290
YAMZIW	10.817	1.295	1.296
YAWXEB	9.866	1.325	1.365
YESLUE	49.024	1.287	1.356
YODXAS	13.856	1.285	1.347
YODXAS01	14.421	1.281	1.355
YODXUM	54.762	1.281	1.37
YODXUM01	54.644	1.275	1.368
ZAMLUU	2.781	1.303	1.344
ZAMMAB	10.435	1.292	1.339
ZAMMEF	4.473	1.305	1.323
ZIKNOW	74.536	1.273	1.365

2.7. Values of single and double bonds according to tabular values used often for tautomer selection

Table S7 Generally accepted values of single and double bonds according to F. H. Allen *et al.*, *J. Chem. Soc. Perkin Trans. II*, **1987**, S1–S19.

Enol-imine tautomer		Keto-amine tautomer	
Car–**C=N**–C# / Å	1.279	**C=C–NH**–C# (Nsp^2 planar) / Å	1.339
Car–OH (in phenols) / Å	1.362	**C=O** (in benzoquinone) / Å	1.230

3. REFERENCES

1   *Philips X'Pert Data Collector 1.3e*, Philips Analytical B. V. Netherlands, 2001**.**
2   *Philips X'Pert Graphic & Identify 1.3e* Philips Analytical B. V. Netherlands, 2001**.**
3   *Philips X'Pert Plus 1.0*, Philips Analytical B. V. Netherlands, 1999**.**
4   Oxford Diffraction (2003), *CrysAlis CCD and CrysAlis RED*. Version 1.170., Oxford Diffraction Ltd, Wroclaw, Poland.
5   G. M. Sheldrick, *Acta Crystallogr*., 2008, **A64**, 112.
6   L. J. Farrugia, WinGX, *J. Appl. Cryst.,* 1999, **32**, 837.
7   Crystallographic data have been deposited with the Cambridge Crystallographic Data Centre, 12 Union Road, Cambridge, CB2 1EZ, UK (fax: +44 1223 336033; e-mail: deposit@ccdc.ac.uk or www: http://www.ccdc.cam.ac.uk). These data can be obtained free of charge from the Director upon request quoting the CCDC deposition numbers 1442712–1442714.
8   L. J. Farrugia, ORTEP-3 for Windows, *J. Appl. Cryst.*, 1997, **30**, 565.
9   C. F. Macrae, I. J. Bruno, J. A. Chisholm, P. R. Edgington, P. McCabe, E. Pidcock, L. Rodriguez-Monge, R. Taylor, J.v.d. Streek and P. A. Wood, *J. Appl. Crystallogr.,* 2008, **41**, 466.
10 STAR^e Software V10.00., Mettler-Toledo AG, 1993- 2011.
11 STAR^e Software V10.00., Mettler-Toledo AG, 1993- 2011.
12 PerkinElmer Spectrum v10.4.2.279, PerkinElmer (2014), PerkinElmer Ltd, United Kingdom.